Author's Accepted Manuscript

Representation of paleomagnetic data in virtual globes (a case study from the Pyrenees)

Tania Mochales, Thomas G. Blenkinsop

Cite this article as: Tania Mochales, Thomas G. Blenkinsop, Representation of paleomagnetic data in virtual globes (a case study from the Pyrenees), *Computers & Geosciences*, http://dx.doi.org/10.1016/j.cageo.2014.05.013

1 **Representation of paleomagnetic data in virtual globes (a case**

2 **study from the Pyrenees)**

3

4 Tania Mochales[a,b], Thomas G. Blenkinsop[c,d]

5 [a]Present Address: Istituto Nazionale di Geofísica e Vulcanologia, Via Arcivescovado 8,

6 67100 L'Aquila, Italy, taniamochales@gmail.com

7 [b]School of Earth Sciences, The University of Queensland, 4072 Brisbane, Australia

8 [c]School of Earth and Environmental Science, James Cook University, 4812 Townsville,

9 Australia.

10 [d]Present Address: School of Earth and Ocean Science, Cardiff University, Main

11 Building, Park Place, Cardiff CF10 3AT, United Kingdom, BlenkinsopT@Cardiff.ac.uk

12

14

15 **Abstract**

16 Virtual globes allow geo-referencing and visualisation of diverse geologic datasets. A

17 vertical axis paleomagnetic rotation study in the Southern Pyrenees, Spain, is used to

18 illustrate the potential of virtual globes for representing paleomagnetic data. A macro

19 enabled workbook that we call P2K, allows KML files to be generated from

20 conventional paleomagnetic datasets. Cones and arch models are used to represent the

21 paleomagnetic vector, and the rotation with regard to the local reference direction,

22 respectively. This visualization provides simultaneous representation of local magnetic

23 declination, inclination and precise confidence cones, shown in their geographic

24 position from diverse perspectives and scales.

25

1. Introduction

Past directions of the Earth's magnetic field are recorded in rocks, and following appropriate paleomagnetic analysis, they can be expressed as a vector (defined by intensity, declination and inclination) with confidence parameters (e.g. Van der Voo, 1990; Opdike and Channel, 1996). Classical representation of paleomagnetic vectors has been limited to 2D. Declination is thus expressed in maps (Figure 1), where authors may represent a local reference direction, and highlight ages or confidence angles, as in Figure 2 (e.g. Holt and Haines, 1993; Govers and Wortel 2005). In other cases, a map is shown with a qualitative palinspastic reconstruction (Figure 1a; e.g. Figure 9 in Speranza et al., 2002) and/or rotation arrows (Figure 1b, e.g. Figure 1 in Antolín et al, 2012 or Figure 1c, e.g. Figure 2 in Govers and Wortel, 2005); contoured plots of rotation angles (Figure 1d, e.g Figure 3 in Titus et al., 2011), or stereoplots of paleomagnetic poles can be also shown (Figure 1e e.g. Figure 6 in Soto et al., 2008). A considerable amount of work has been performed to compile paleomagnetic data in order to interpret tectonics, such as the Global Paleomagnetic database, (McElhinny and Lock, 1996) or MagIC (Tauxe et al., 2012). The Pyrenean Paleomagnetic Database (Lòpez et al., 2008; San Miguel et al., 2010; Pyrenean Pmag DB, IGME) is the first paloemagnetic dataset conceived at the orogen scale using geologic maps as the main background.

During the last few years virtual globes have been adopted in response to the needs of the scientific, pedagogic and industrial communities (e.g. SERC, Pedagogy in Action; World Wind, NASA). Virtual globes can geo-reference geologic datasets as diverse as maps and cross-sections (Google Earth profile, De Paor and Whitmeyer, 2011), world magnetic declination (Google Compass), coal exploitation (e.g. Queensland Coal

51   Mines, Queensland Government Department of Natural Resources, Mines and Water;

52   Vizmap, Google Earth Applications), dams and freshwater lakes (e.g. SEQ Water,

53   Geospatial Information and Technology Association [GITA]; Vizmap, Google Earth

54   Applications), and geological mapping (SIGECO, Instituto Geológico y Minero de

55   España) among others, which testify to the versatility and widespread use of this tool.

56   Virtual globes have become very helpful in structural geology visualization (Simpson

57   and De Paor, 2009; De Paor and Whitmeyer, 2011; Blenkinsop, 2012; Martínez-Torres

58   et al., 2012) since they can display topography and geology, and allow quick shifts of

59   user's viewpoint and scale. Based on this background, we intend that paleomagnetic

60   data be included among the geological datasets that can be represented in Google Earth.

61

62   The open-source Keyhole Markup Language (KML) represents a great advance for

63   virtual globes. KML is an XML-based language that manages the display of 3D

64   geospatial data, which has become widespread in scientific research relying on virtual

65   globes (De Paor et al., 2012). KML enables users to customize data in ways as varied as

66   Shapefiles in ArcGIS. These capacities are possible in combination with COLLADA

67   (COLLAborative Design Activity) models, generated, for example by SketchUp and

68   other 3D modelling applications (De Paor and Whitmeyer, 2011). In this paper we used

69   the free SketchUp (now SketchUp Make) application to create a symbology for

70   representing paleomagnetic data in virtual globes.

71

72   We propose a protocol for the symbology that achieves a clear distinction between

73   clockwise and anticlockwise paleomagnetic rotations (Figure 3), and normal and reverse

74   polarity, as well as an indication of the confidence parameters. These data can be easily

75   and well represented in a virtual globe, providing not only information about declination

76 but also inclination (often omitted from 2D representations). A local reference direction

77 can also be shown for any rotation. We provide a macro-enabled spreadsheet (P2K) that

78 expresses the paleomagnetic data using the symbology via a KML file, allowing it to be

79 presented and displayed in bird's eye views and through 360º viewpoints in virtual

80 globes. Pop-ups with numerical and bibliographic information are included. This

81 approach allows easy visualisation and compilation of paleomagnetic data, promoting

82 the creation of geo-referred databases. We illustrate the method with a case study from

83 the Pyrenees.

84

85 **2. Case Study: The Boltaña Anticline**

86 The Boltaña anticline, in the Southern Pyrenees, is a 25 km long, north-south oriented

87 fold located westwards of the South Pyrenean central Unit (SPCU), which is a thrust-

88 and-fold system transported south in piggyback sequence during Eocene times

89 (Puigdefàbregas et al., 1975). Contemporary with the slow westwards propagation of

90 south-transported thrust sheets, numerous structures transverse to the Pyrenean trend

91 (WNW-ESE) were formed, such as the Boltaña anticline. The strata involved were

92 coevally deposited through Eocene times, including a pre-folding stage of limestones in

93 a platform sequence (56-49 Ma), overlain by slope rocks in an incipient synfolding

94 setting in the Boltaña anticline (49-43 Ma). Next, deltaic progradation occurred through

95 the eastern flank of the Boltaña anticline (43-41 Ma), followed by continental

96 deposition (41-35 Ma) (Mochales et al., 2012a and references therein). Lutetian to

97 Bartonian sediments (49-38 Ma) with growth-strata geometries record successive non-

98 coaxial deformational episodes. Firstly, the folding of the Boltaña anticline took place

99 ~43 Ma (Lutetian, Puigdefàbregas, 1975; Fernández et al., 2004; Mochales et al., 2010;

100 Muñoz et al., 2013). Later, a clockwise rotation of the Boltaña thrust sheet, during 41-

101 35 Ma, explains the obliquity of the anticline with respect to the Pyrenean trend

102 (Mochales et al., 2012b). Exposure is excellent, and the area has an acceptable Google

103 Earth aerial image and DEM, making for a very suitable case study.

104

105 **3. Representation of paleomagnetic data in virtual globes**

106 Previous works that visualized structural geology data (e.g. Whitmeyer et al., 2010;

107 Blenkinsop, 2012), opened new perspectives in virtual globe visualization and inspired

108 the creation of paleomagnetic symbols in SketchUp (available freely from Trimble now

109 as SketchUp Make) in this study, using COLLADA models like those created for

110 representing structures.

111

112 Paleomagnetic data are usually organized in spreadsheets for final representation on

113 digital maps, analysis and interpretation. Data should meet several reliability criteria

114 such as laboratory, processing and statistical procedures as well as geological and

115 geomagnetic constraints (Van der Voo, 1990; Fisher, 1953). They are then commonly

116 compiled in rows where intensity of the magnetization and paleomagnetic vectors from

117 the coordinate reference system (in situ) to the paleogeographical one (bedding

118 correction) is shown (declination and inclination). Confidence angles (α95), and

119 paleopoles corresponding to the age of the case study and author of the site are also

120 documented.

121

122 The COLLADA models used to represent the paleomagnetic data (Figure 3) permit

123 visualisation in virtual globes more intuitively than standard map symbols. The models

124 were created in SketchUp, and are provided in supplementary information with this

125 paper (Appendix A). The models consist of two cones, one to represent the

126 paleomagnetic remanent vector, and one to show the confidence cone. The models are

127 3D representations of a common 2D paleomagnetic symbol. The cones are transparent

128 so that they do not disturb the background, and encompass α95 from 1º to 60º,

129 indicating the semi-angle of confidence from Fisher (1953) statistics. The models have

130 long dimensions of 16 m, appropriate to an outcrop scale. These cones are duplicated to

131 represent reverse or normal polarity with black or white versions respectively. The

132 cones are shown elevated above the ground surface, and the base of the cone is

133 connected to the ground at the observation site with a vertical line, allowing a clearer

134 visualization of the background. The size of the cones and their height are adjustable in

135 P2K according to the scope of the work.

136

137 The greatest advantage of this 3D representation compared to previous 2D methods is

138 that the inclination component of the paelomagnetic vector of each site can be

139 visualised, and with respect to the local reference direction. Classical 2D representations

140 only allow visualization of the declination of the paleomagnetic vector, concealing the

141 inclination component, which can be highly disturbed, especially when differential

142 lithostatic loading produces inclination errors (Bilardello and Kodama, 2010). The

143 greater ease of examining the inclination affords new insights into the degree of

144 magnetic inclination perturbation throughout the rotational process. Quick assessment

145 of inclination anomalies with regard to the paleopole characteristic of the geological

146 time in question can be made (Figure 4). Another interesting advantage is the proper

147 representation of the α95 confidence cone, which has a 3D attribute and is usually

148 incorrectly projected in a 2D plane. A correction factor has to be introduced to the

149 rotation error (Demarest, 1983) to represent the projection of a95 in a plane properly.

150 Alternatively, the equation α95/cos (Inc) can accurately determine the 2D projection of

151   α95 (Butler, 1992). Both calculations can be avoided by the correct representation of

152   the error in 3D. This representation of paleomagnetic data in 3D is especially effective

153   in combination with representation of structural data (e.g. S2K, Blenkinsop, 2012),

154   which allows a first glance at the relationship between structural and paleomagnetic

155   directions (Figure 5).

156

157   It is also useful to have a direct representation of vertical axis rotations with regard to

158   the local reference direction. In P2K this is possible using an arch model, in which a

159   curved arrow (arch) shows the rotation, distinguished by colour between clockwise and

160   anticlockwise rotations. By means of the case study of the Boltaña anticline we can

161   illustrate variations in the amount of vertical axis rotation (Figure 4). The younger sites,

162   located towards the south, underscore the more striking rotation corresponding to the

163   Priabonian age. Figure 4 shows the difference between the northwestern (older) sites,

164   that underwent around 40º of rotation, compared to the southeastern sites (younger) that

165   are closer to the Eocene reference (close to the current magnetic north) and therefore

166   less rotated.

167

168   **4. Data Input and KML file generation with P2K**

169   The P2K spreadsheet can be downloaded from the Journal web site (Appendix A). It

170   requires Excel in a macro-enabled version, and it is usable in any operating system that

171   can run Excel. Two versions are offered: P2K.xlsm works with Excel 2011 for

172   Macintosh and Windows, while P2K.xls works for Excel 2007 for Windows and Excel

173   2004 for Macintosh. The paleomagnetic input data are: Site name, Geographic

174   coordinates, Rotation angle, Inclination, α95 confidence angle, Polarity, Author,

175   Direction of paleomagnetic reference North, and inferred clockwise (C) or

7

176   anticlockwise (A) direction of rotation. UTM coordinates are optional. Normal (N) and

177   Reverse (R) polarities are accepted, as well as normalized polarity: antipodal Reverse

178   polarity (-R). These normalized polarities are used when poles correspond to the

179   antipodal direction of the majority of the dataset, making the normal and reverse

180   directions commensurate.

181

182   The organisation of the P2K spreadsheet is as follows. In the first row, cell A2 contains

183   a name that is used for folders within the KML document, which takes the name of the

184   spreadsheet. Cell A4 contains a value for a scale, which multiplies the 16 m dimension

185   of the cones symbol to an appropriate value if necessary. Cell A6 contains a height

186   value that sets the height of the symbol above the ground level in metres. Data entry

187   begins in row 3. The first column of cells corresponds to the site label. The next four

188   columns correspond to the geographic coordinates (second and third in UTM, forth and

189   fifth in decimal degrees). Coordinate information must be entered in WGS84 datum

190   because that is the datum used by Google Earth. The sixth and seventh columns

191   correspond to the Declination and Inclination angles. The $\alpha 95$ angle is located in the

192   eighth column, polarity in the ninth and source author in the tenth. The reference

193   declination and sense of rotation are entered in the final two columns. The

194   paleomagnetic information can be read in a pop-up balloon.

195

196   The code necessary to represent the paleomagnetic information by generating a KLM

197   file resides in the macro of the spreadsheet, which can be run from the Macro menu.

198   The macro creates a KML file with three folders: the first is called *Symbol* and refers to

199   the cones that represent the remanent paleomagnetic vectors. The second (*Data*) refers

200   to the information that is displayed in the balloons, and the site names. The third

201 (*Rotation symbol*) refers to the arch symbol that indicates the vertical axis rotation. Each

202 of the folders can be turned on and off independently in the Places panel of Google

203 Earth.

204

205 The KML document calls on the *Symbols* and *arches* models that are kept in folders of

206 ~~that name~~. The P2K spreadsheet and these folders must be placed in a single folder on

207 the user's computer storage. The P2K folder supplied contains the P2K.xls and

208 ~~P2Kxlms~~ spreadsheets, the Boltañaexample.kml example, and the symbols and arches

209 folders. P2K ReadMe contains more detailed instructions about running the macro.

210

211 An alternative approach could be to enter data into a Fusion Table linked to a PHP,

212 Python or Ruby script, which could output the Google Earth API embedded in a web

213 page (De Paor et al., 2012). The macro code could also be adapted to generate the kml

214 files with other applications that implement Visual Basic.

215

216 **5. Conclusions**

217 Virtual Globes are increasingly used by geologist to represent field data. They are a

218 quick and economic way to store and share information. P2K is a macro-enabled Excel

219 workbook to generate KLM files from paleomagnetic data, for visualization in virtual

220 globes. Advantages of representing paleomagnetic data in the manner proposed here are

221 visualisation of both declination and inclination simultaneously, accurate representation

222 of confidence cones, and the ability to examine data sets in their geographic context

223 with rapid change of scale and perspective.

224

225

226

227

228 **Acknowledgements**

229 TM acknowledges one-year postdoctoral fellowship from ARC-DP0986762 project

230 (UQ) and current researcher contract from FIRB-ABRUZZO (INGV). We are also

231 grateful to Juanjo Villalaín for his advice on this work. Mark Stokes put in a great effort

232 to create the SketchUp models of the arches. Detailed comments from Emilio L. Pueyo

233 and two other anonymous reviewers are appreciated.

234

235 **Appendix A. Supporting Information**

236

237 **Supplementary data associated with this article – the P2K folder – can be found in**

238 **the online version at**

239

240 **References**

241 Antolín, B., Appel, E., Gloaguen, R., Dunkl, I., Ding, L., Montomoli, C., Liebke, U.,

242   Xu, Q., 2010, Paleomagnetic evidence for clockwise rotation and tilting in the

243   eastern Tethyan Himalaya (SE Tibet): Implications for the Miocene tectonic

244   evolution of the NE Himalaya. Tectonophysics 493, 172-186.

245 Bentham, P.A., 1992. The tectono-stratigraphic development of the western oblique

246   ramp of the south-central Pyrenean thrust system, Northern Spain. Ph.D. thesis,

247   University of Southern California. 253 p.

248 Blenkinsop T.G., 2012, Visualizing structural geology: From Excel to Google Earth,

249   52-56. In Computers & Geosciences, 45, 52-56.

250   Butler, R.F., 1992, Paleomagnetism, Magnetic Domains to Geologic Terranes, Boston,

251   Blackwell, 319 p.

252   COLLADA, COLLAborative Design Activity. http://www.khronos.org/collada/

253   (accessed 6.3.14)

254   De Paor, D., Whitmeyer, S.J., 2011, Geological and geophysical modelling on virtual

255   globes using KML, COLLADA, and Javascript. Computers and Geosciences 37,

256   100–110.

257   De Paor, D., Whitmeyer, S.J., Marks, M., Bailey, J.E., 2012, Geoscience applications of

258   client/server scripts, Google Fusion Tables, and dynamic KML. Geological

259   Society of America Special Papers, 492, p. 77-104. doi: 10.1130/2012.2492(06)

260   Demarest, H.H., 1983, Error analysis for the determination of tectonic rotation from

261   paleomagnetic data. Journal of Geophysical Research, 88, B5, 4321-4328.

262   Fernández, O., Muñoz, J.A., Arbués, P., Falivene, O., Marzo, M., 2004, Three-

263   dimensional reconstruction of geological surfaces: an example of growth strata

264   and turbidite systems from the Ainsa Basin, Pyrenees, Spain. American

265   Association of Petroleum Geologists Bulletin 88 (8), 1049-1068.

266   Fisher, R.A., 1953. Dispersion on a sphere. Proc. R. Soc. London Ser. A 217, 295-305.

267   Google Compass. http://googlecompass.com/ (accessed 22.4.14)

268   Google Earth Profile. http://library.usask.ca/murray/data-and-

269   gis/GISpages/HowdoIfolder/HowdoIelevationinGoogleEarth.pdf (accessed

270   22.4.14)

271   Govers, R. and Wortel, M.J.R., 2005, Lithosphere tearing at STEP faults: Response to

272   edges of subduction zones. Earth and Planetary Science Letters, 236, 505– 523.

273   Holt, W.E., and Haines, A.J., 1993, Velocity fields in deforming Asia from the

274   inversion of earthquake-released strains: Tectonics, v. 12, p. 1–20.

275   Bilardello, D., Kodama, K.P., 2010, A new inclination shallowing correction of the

276   Mauch Chunk Formation of Pennsylvania, based on high-field AIR results:

277   Implications for the Carboniferous North American APW path and Pangea

278   reconstructions, Earth Planet. Sci. Lettrs., 299, 218-227.

279   KML, World Wide Web Consortium. http://www.w3.org/(accessed 22.4.14)

280   Krijgsman, W., and Tauxe, L., 2004, Shallow bias in the Mediterranean palaeomagnetic

281   directions caused by inclination error. Earth and Planetary Science Letters 222

282   (2), 685–695.

283   López, M.A., Oliván, C., Oliva, B., Pueyo, E.L. and the GeoKin3DPyr group, 2008.

284   Pyrenean paleomagnetic databases. Geotemas, 10, 1219-1222.

285   Martínez-Torres, L.M., Lopetegui, A., Eguiluz, L., 2012, Automatic resolution of the

286   three-points geological problem. Computers & Geosciences, 42, 200-202.

287   Mattei, M., Cifelli, F., D'Agostino, N., 2007, The evolution of the Calabrian Arc:

288   Evidence from paleomagnetic and GPS observations. Earth and Planetary Science

289   Letters 263, 259–274

290   McElhinny, M.W. and Lock, J., 1996, IAGA paleomagnetic databases with Access,

291   Surv. Geophys.,17,575-591.

292   Mochales, T., Pueyo, E.L., Casas, A.M., Barnolas, A., Oliva-Urcia, B., 2010.

293   Anisotropic magnetic susceptibility record of the kinematics of the Boltaña

294   Anticline (Southern Pyrenees): Geological Journal, v. 45, p. 562-581, doi:

295   10.1002/gj.1207

296   Mochales, T., Barnolas, A., Pueyo, E.L., Serra-Kiel, J., Casas, A.M., Samsó, J.M.,

297   Ramajo, J., Sanjuán, J., 2012a, Chronostratigraphy of the Boltaña anticline and

298   the Ainsa Basin (Southern Pyrenees). Geological Society of America Bulletin.

299   doi:10.1130/B30418.1.

300   Mochales, T., Casas, A.M., Pueyo, E.L., Barnolas, A., 2012b, Rotational velocity for

301   oblique structures (Boltaña anticline, Southern Pyrenees). Journal of Structural

302   Geology 35 (2012) 2-16. doi:10.1016/j.jsg.2011.11.009.

303   Mümtaz Hisarlı, Z., 2011, New paleomagnetic constraints on the late Cretaceous and

304   early Cenozoic tectonic history of the Eastern Pontides. Journal of Geodynamics,

305   52, Issue 2, 114–128.

306   Muñoz, J.A., Beamud, B., Fernández, O, Arbués, P., Dinarès-Turell, J., Poblet, J., 2013,

307   The Ainsa fold and thrust oblique zone of the central Pyrenees: Kinematics of a

308   curved contractional system from paleomagnetic and structural data. Tectonics 32

309   (59), 1142-1175.

310   Opdike, N.D, Channell, J.E.T., 1996, Magnetic Stratigraphy. International Geophysical

311   Series, 64, Academic Press, San Diego. 346 pp.

312   Puigdefàbregas, C. ,1975, La sedimentación molásica en la cuenca de Jaca. Pirineos

313   104, 1–188.

314   Pyrenean Pmag DB. http://www.igme.es/infoigme/aplicaciones/paleomag (accessed

315   22.4.14)

316   Queensland Coal Mines, Queensland Government Department of Natural Resources,

317   Mines and Water; Vizmap, Google Earth Applications. Vizmap, Google Earth

318   Applications.   http://www.vizmap.com.au/services/google-earth-applications/

319   (accessed 22.4.14)

320   San Miguel, G., Hernández, R., Pueyo, E.L. and the Geokin3DPyr, 2010, Pyrenean

321   Paleomagnetic Database; Concept, state-of-the-art, and web interface design.

322   Proceedings MAGIBER VI, 50-53.

323   SERC, Pedagogy in Action. http://serc.carleton.edu/sp/library/google_earth/how.html

324   (accessed 22.4.14)

325   SEQ Water, Geospatial Information and Technology Association [GITA]; Vizmap,

326   Google Earth Applications. Vizmap, Google Earth Applications.

327   http://www.vizmap.com.au/services/google-earth-applications/ (accessed

328   22.4.14)

329   SIGECO, Instituto Geológico y Minero de España, Ministerio de Economía y

330   Competitividad. http://cuarzo.igme.es/sigeco/Default.aspx (accessed 6.3.14)

331   Simpson, C., De Paor, D.G., 2009, Restoring maps and memoirs to four-dimensional

332   space using virtual globe technology: a case study from the Scottish Highlands.

333   In: Law, R.D., Butler, R.W.H., Holdsworth, R.E., Krabbendam, M., Strachan,

334   R.A. (Eds.), Continental Tectonics and Mountain Building: The Legacy of Peach

335   and Horne, 335. Geological Society of London Special Publication, pp. 427–439.

336   Speranza, F., Villa, I.M., Sagnotti, L., Florindo, F., Cosentino, D., Cipollari, P., Mattei,

337   M., 2002, Age of the Corsica-Sardinia rotation and Liguro-Provencal Basin

338   spreading: New paleomagnetic and Ar/Ar evidence. Tectonophysics 347: 231-

339   251. doi:10.1016/S0040-1951(02)00031-8.

340   Soto, R., Villalaín J.J., Casas-Sainz, A.M,, 2008, Remagnetizations as a tool to analyze

341   the tectonic history of inverted sedimentary basins: A case study from the Basque-

342   Cantabrian basin (north Spain). Tectonics, Vol. 27, TC1017,

343   doi:10.1029/2007TC002208, 2008

344   Taberner, C., Dinarés-Turell, J., Jiménez, J., Docherty, C., 1999, Basin infill

345   architecture and evolution from magnetostratigraphic cross-basin correlations in

346   the southeastern Pyrenean foreland basin: Geological Society of America Bulletin,

347   11(8), p. 1155-1174.

348   Tauxe, L., Constable, C.G., Jarboe, N., Koppers, A.A.P., Minnett, R., Shaar, R., 2012,

349   PmagPy: Software package for paleomagnetic data analysis and gateway to the

350   Magnetics Information Consortium (MagIC) Database. Geochemistry,

351   Geophysics, Geosystems doi: 10.1029/0000.

352 Titus, S.J., Crump, S., McGuire, Z., Horsman, E., Housen, B., 2011, Using vertical axis

353   rotations to characterize off-fault deformation across the San Andreas Fault

354   system, central California. Geology 39: 711-714.

355 Van der Voo, R., 1990, The reliability of paleomagnetic data. Tectonophysics 184, 1-9.

356 Vizmap, Google Earth Applications. http://www.vizmap.com.au/services/google-earth-

357   applications/ (accessed 22.4.14)

358 Whitmeyer, S.J., Nicoletti, J., De Paor, D.G., 2010, The digital revolution in geologic

359   mapping. GSA Today: A Publication of the Geological Society of America, vol.

360   20, doi:10.1130/GSATG70A.1.

361 World Wind, NASA. http://goworldwind.org/demos/(accessed 22.4.14)

362

363 **Figure Captions**

364 Figure 1. Ways of displaying paleomagnetic information in the literature. a)

365 Paleomagnetic vectors shown with palinspastic reconstruction, modified ~~form~~ Speranza

366 et al., (2002); b) Paleomagnetic vectors shown as vertical axis ~~rotation~~ with respect to

367 the north, modified from Antolín et al., (2012); c) Rotation symbols show the regionally

368 observed sense of motion on transform faults, or paleomagnetic rotations about a

369 vertical axis, from Govers and Wortel, (2005). d) Paleomagnetic group means are

370 superimposed over contoured rotation maps, from Titus et al., (2011). e) Equal area

371 projections showing the site-mean paleomagnetic directions with their associated a95,
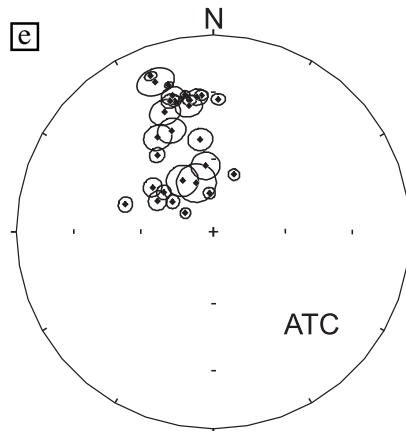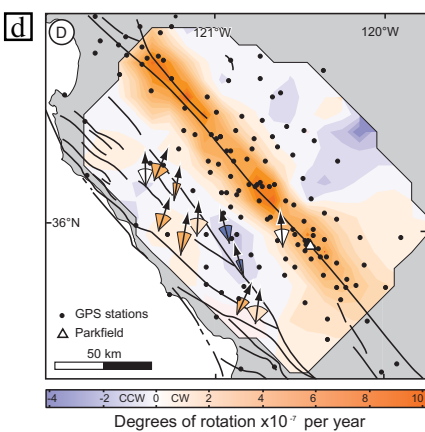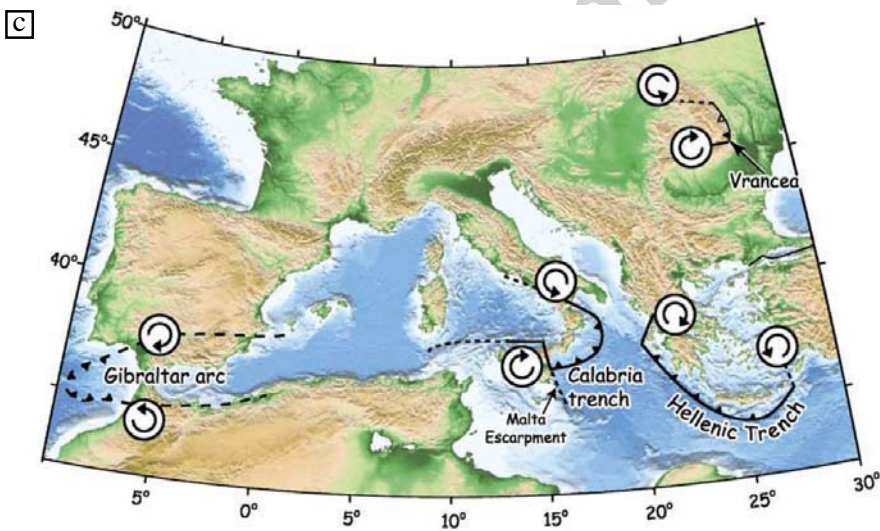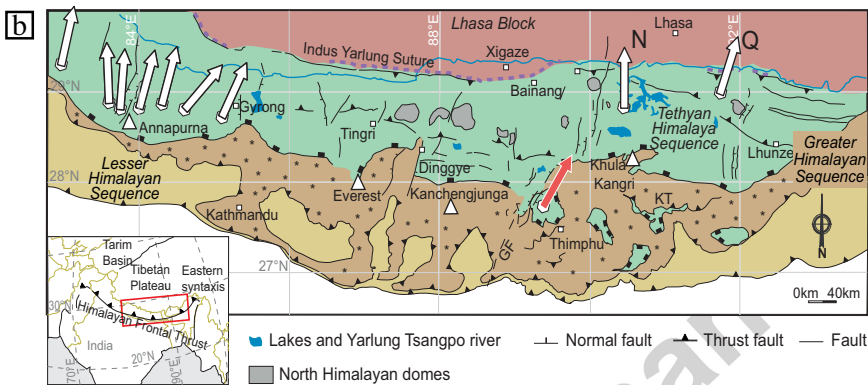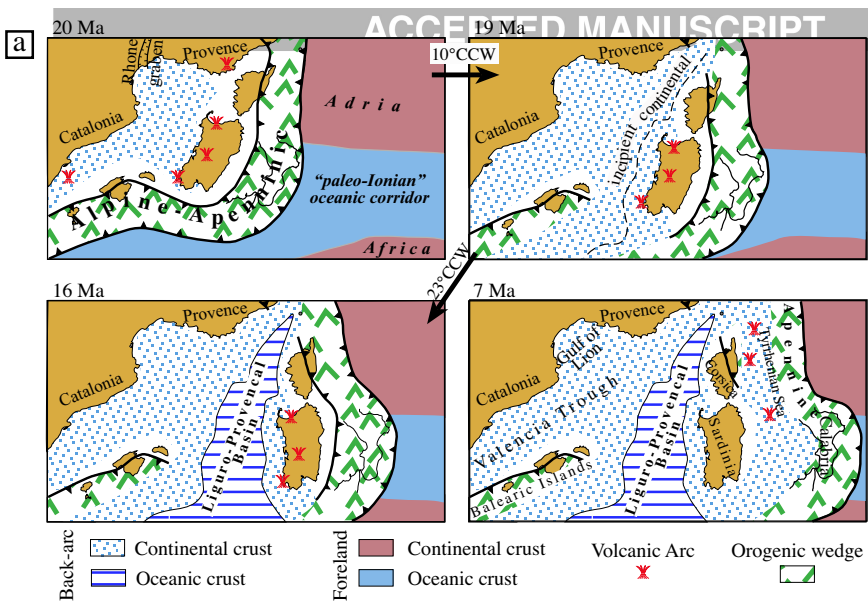
372 from Soto et al., (2008).

373 Figure 2. Rotations in map view (arrows represent the magnetic declination and the

374 confidence angle), modified from Mochales et al. (2012b).

375 Figure 3. Examples of models created in SketchUp. Rotation is the angle difference

376 between the local declination and the local reference direction. Due to 3D

377 representation, we can illustrate inclination and the α95 confidence angle correctly.

378 Figure 4. Boltaña anticline case study. Normal polarities (black arrows) plunge into the

379 earth in the northern hemisphere and reverse polarities (white arrows) emerge from the

380 earth. Here, reverse polarities have been normalized (-R) to be comparable with others

381 and an Eocene reference (Taberner et al., 1999). A rotation can be appreciated in

382 younger materials (Priabonian) towards the southeast, as well as inclination and

383 confidence angle of each site. The figure illustrates the area where the rapid vertical axis

384 rotation was detected from map view (a), oblique view (b) and horizontal view (c)

385 Figure 5. Oblique view of a northern area where paleomagnetic data (P2K) and

386 structural data (SK2) are here combined to get a realistic understanding of the

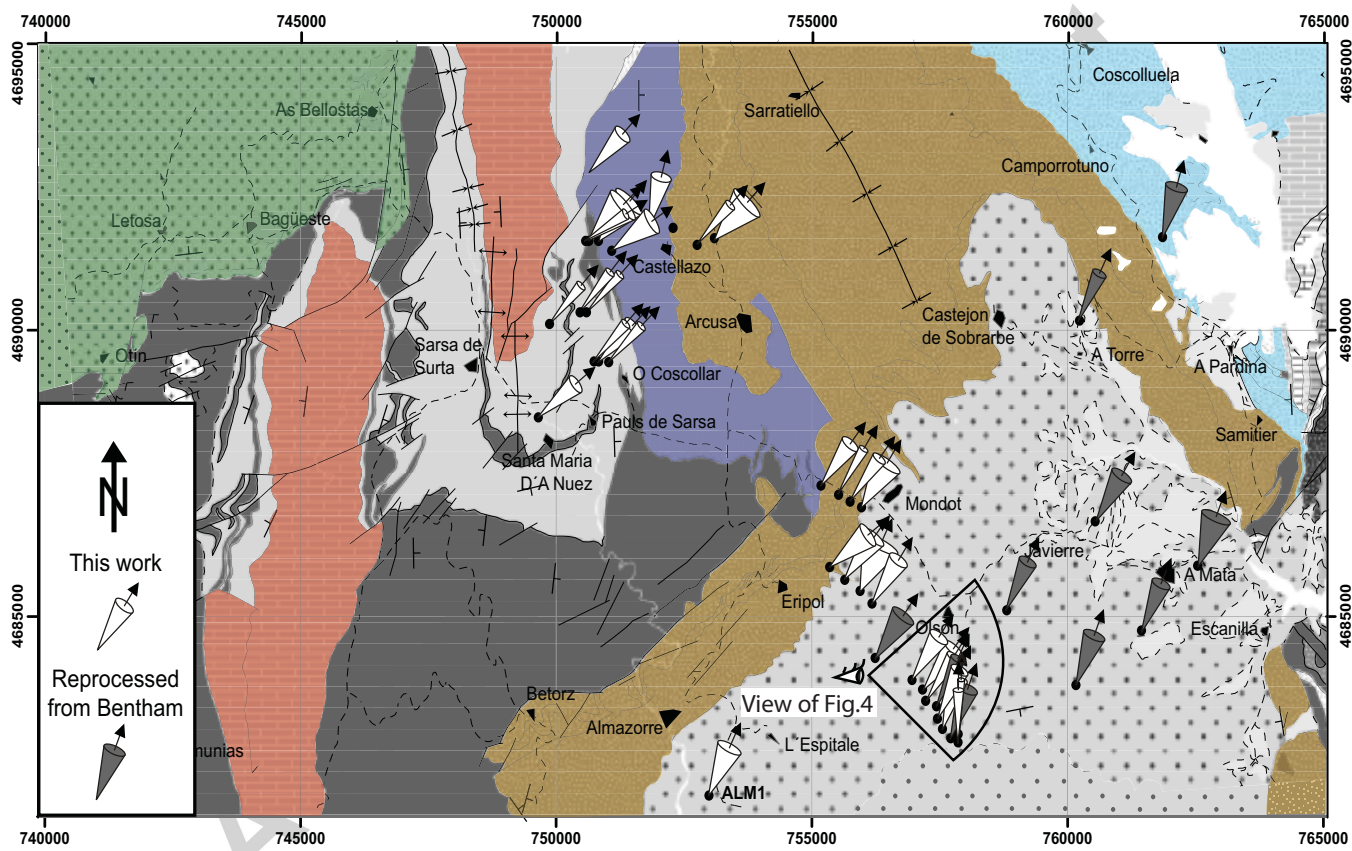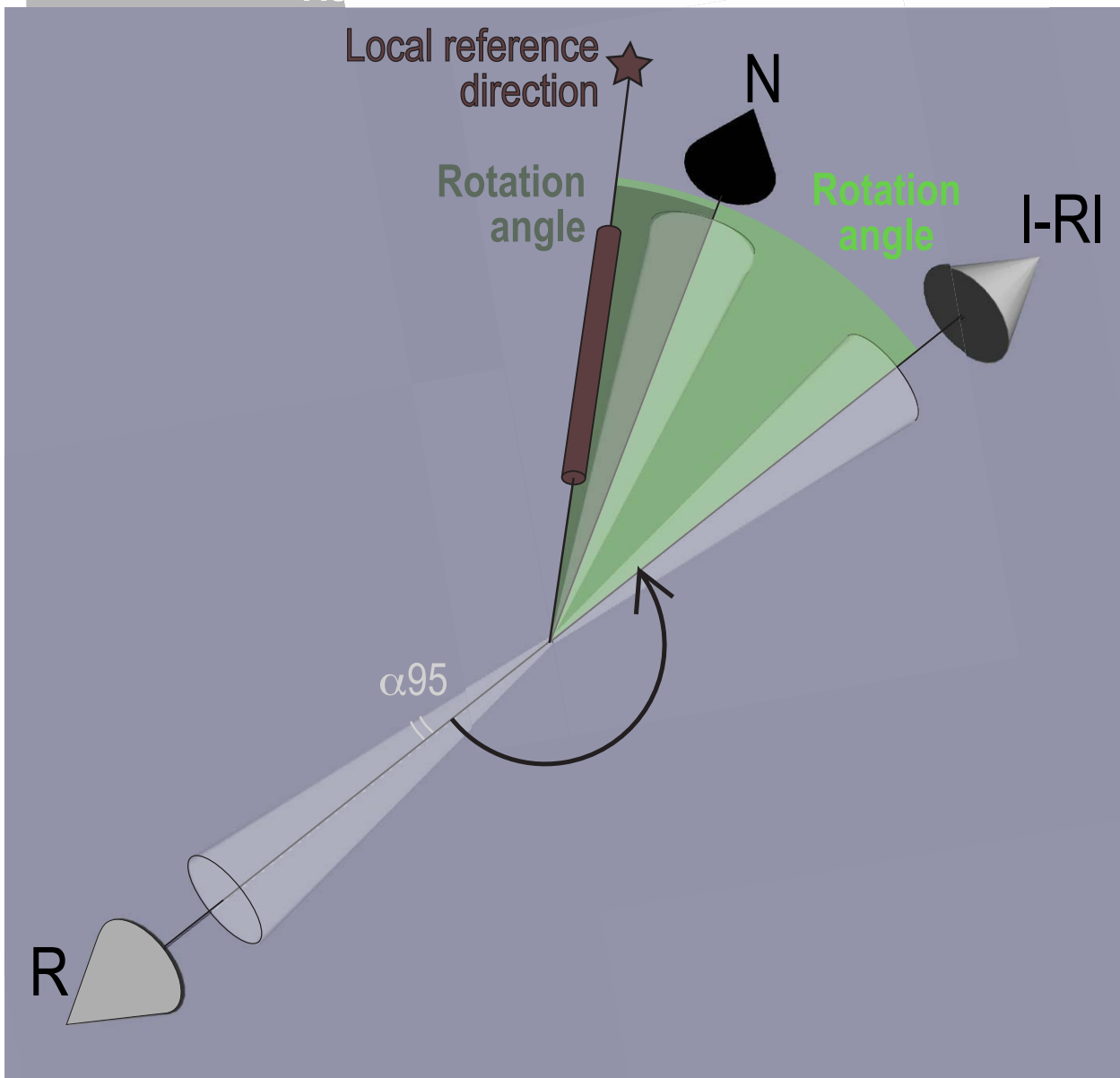387 paleomagnetic and tectonic record.

Figure 1

Figure 2

Figure 3

Figure 4

ACCEPTED MANUSCRIPT

Site ESC6

Declination = -3 °

Inclination = 47°

Alpha95 = 7°

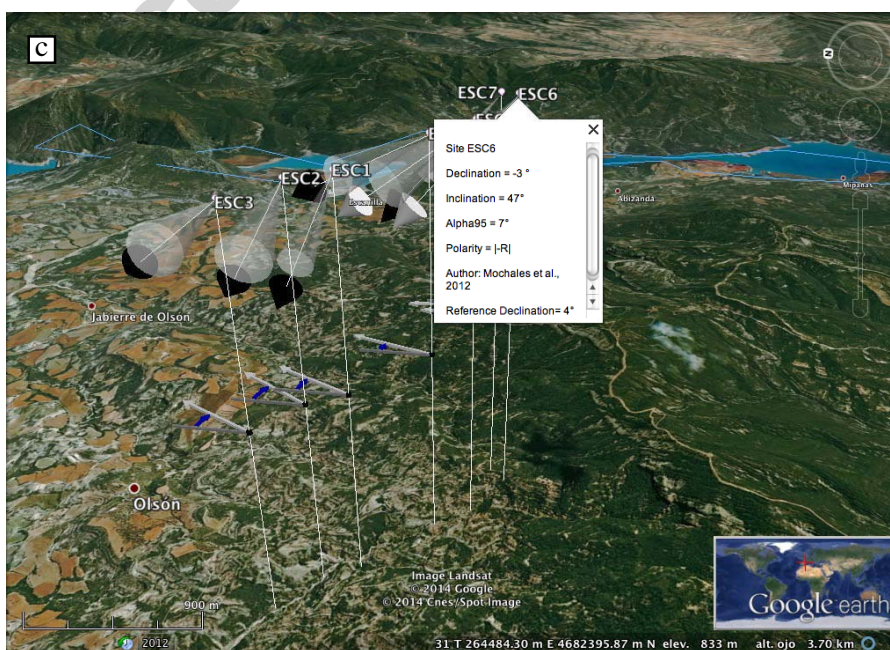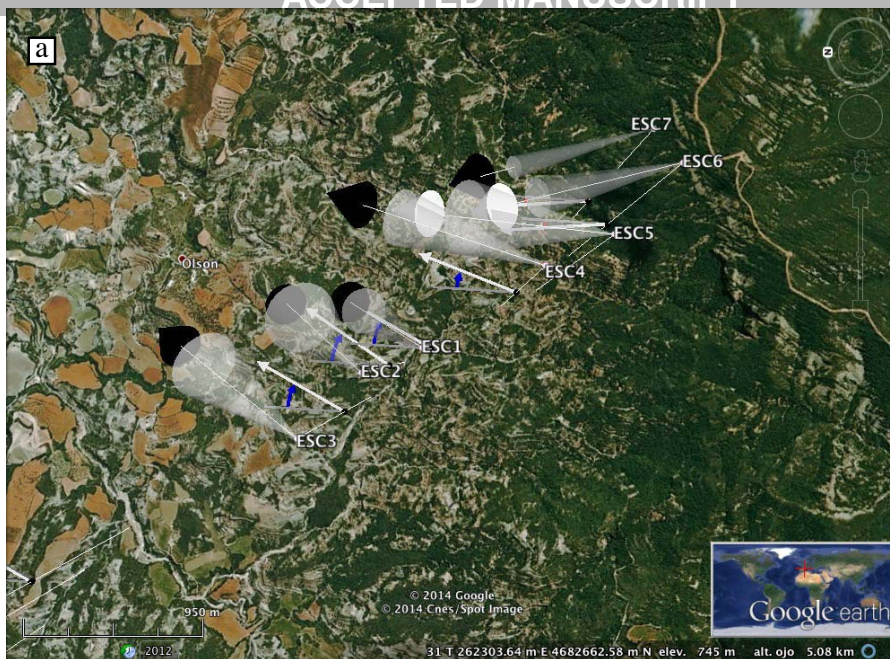Polarity = |-R|

Author: Mochales et al., 2012

Reference Declination= 4°

Figure 5

Paleomagnetic vectors in 3D